Crop Leaf Area Index Retrieval Based on Inverted Difference Vegetation Index and NDVI

Yuanheng Sun, Huazhong Ren, Tianyuan Zhang, Chengye Zhang, and Qiming Qin

***Abstract*— Leaf area index (LAI), an important parameter describing a crop canopy structure and its growth status, can be estimated from remote sensing data by statistical methods involving vegetation indices (VIs). This letter reports the development of a new VI, the inverted difference vegetation index (IDVI), for crop LAI retrieval. The IDVI can overcome the saturation issue of the normalized difference vegetation index (NDVI) at high LAI values and exhibits robust insensitivity to crop leaf water and chlorophyll content. By combining the IDVI and NDVI with a scaling factor, we constructed a novel statistical regression model with parameters that can be calibrated to a specific region to estimate the LAI. Validations on simulated data and *in situ* observations show that the proposed retrieval method with the IDVI is stable for low and high LAIs and obtains better results than the empirical method involving the NDVI at the regional scale. Findings in this letter will benefit future agricultural applications.**

***Index Terms*— Crop, inverted difference vegetation index (IDVI), leaf area index (LAI), normalized difference vegetation index (NDVI), sensitivity analysis.**

I. Introduction

LEAF area index (LAI), a key indicator of a crop canopy structure and growing status, provides crucial information on health diagnosis, yields prediction and other practical agriculture applications. Based on the parts of vegetation which are accounted, it could be defined as the green area including the stem and wilted leaf [plant area index (PAI)] or the purely green leaf area [1]. Conventional crop LAI acquisition depends on ground-based measurements, which is relatively accurate but labor-intensive and often inefficient [2]. Remote sensing offers a quick and convenient approach for estimating the crop LAI across wide areas and has been used widely in LAI mapping for croplands [3].

Multispectral imageries, such as data from Landsat-8/OLI and Sentinel-2/Multispectral Instrument (MSI), remain the most practical commonly used data source in the remote sensing crop LAI estimation. Time series data collected over 40 years, together with forthcoming high-temporal resolution imageries, provide abundant information with which to improve the modeling of the LAI retrieval. Numerous precision farming applications, such as crop irrigation management, within-field fertilization, and time determination for harvest, will greatly benefit from these improvements. Retrieving LAI from the multispectral imagery can be roughly grouped into two types [4]. The first type comprises statistical methods derived from spectral VIs [5]. The second type encompasses the physical retrieval models that usually simulate the spectral and bidirectional canopy reflectance by using a radiative transfer model first and then reverse LAI with the known reflectance and other auxiliary information [6]. The statistical methods are convenient for the development and effectiveness of calculations and, thus, widely used in regional applications. However, the applicable statistical method depends on the variability and quality of data used in the model calibration. To refine the results, research works on calibration at different times, sites, and biomes have been conducted to stabilize the specific statistical relationship between the LAI and VIs [7], [8].

Besides site and biome calibration issues, other problems that limit the accuracy of statistical models in estimating LAI remain. Some widely used VIs, such as the normalized difference vegetation index (NDVI) and the soil-adjusted vegetation index (SAVI), become saturated when the LAI is sufficiently high (i.e., LAI $>$ 2) [9]. Thus, the resulting estimations retain some uncertainty, even at the regional scale with site-specific calibration. This letter focuses on two topics to weaken the influence of the saturation issue on the crop LAI estimation from the statistical methods. First, a robust and stable VI that is sensitive to the LAI changes at high LAI ranges but insensitive to other factors is necessary. Second, the weighted ratio of the optimal VIs for the LAI estimation should be adaptive and robust to the LAI changes.

To address the saturation issue, this letter first proposes the inverted difference vegetation index (IDVI) to circumvent the saturation of the NDVI at high LAI. Analyses of the sensitivity and the time series of the index are discussed thereafter. A scale factor is then introduced to combine the NDVI and IDVI for the overall LAI retrieval process based on the multiple channels in the Sentinel-2A Multispectral Instrument. Finally, the retrieval results are validated against the simulated and *in situ* LAI observation data.

II. Data Collection

A. Simulated Canopy Reflectance

The crop canopy spectral reflectance and its corresponding LAI value are required in developing and analyzing the

Manuscript received April 3, 2018; revised June 21, 2018 and July 13, 2018; accepted July 13, 2018. Date of publication August 9, 2018; date of current version November 5, 2018. This work was supported in part by the Natural Science Foundation of China under Grant 41771371 and Grant 41771369, in part by NSFC and STFC of the U.K. Joint Program Project under Grant 61661136006002, and in part by the China National Major Project of High-Resolution Earth Observation under Grant 11-Y20A05-9001-15/16. *(Corresponding authors: Huazhong Ren; Qiming Qin.)*

The authors are with the Institute of Remote Sensing and Geographic Information System, Peking University, Beijing 100871, China, also with the Beijing Key Laboratory of Spatial Information Integration and 3S Application, Peking University, Beijing 100871, China, and also with the Engineering Research Center for Geographical Information Basic Softwares and Applications, State Bureau of Surveying and Mapping, Beijing 100871, China (e-mail: renhuazhong@pku.edu.cn; qmqin@pku.edu.cn).

Color versions of one or more of the figures in this letter are available online at http://ieeexplore.ieee.org.

Digital Object Identifier 10.1109/LGRS.2018.2856765

TABLE I
NOMINAL VALUES OR RANGE OF PARAMETERS USED IN THE PROSAIL MODEL

Input parameters	Nominal values or ranges
Cab (chlorophyll content, μg/cm^2)	23.0 - 63.0
Car (carotenoids content, μg/cm^2)	*Cab*/5
Cw (water content, g/cm^2)	0.005 - 0.045
Cm (dry matter content, g/cm^2)	0.003 - 0.008
N (Leaf mesophyll structure index)	1.0 - 2.0
LAI (Leaf area index, m^2/m^2)	0.1 - 6.0
ALA (Average leaf angle, °)	35 - 65
SZA (Sun zenith angle, °)	20 - 60
OZA (Observation zenith angle, °)	0 - 40

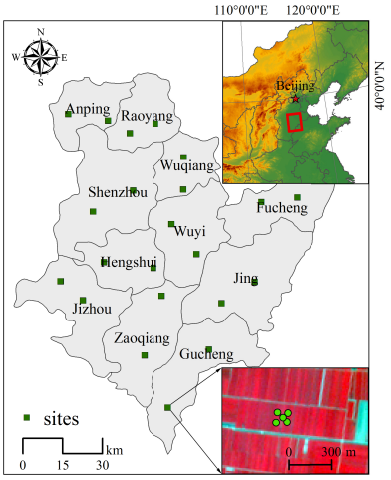

Fig. 1. Location of Hengshui in the North China Plain and the distribution of LAI measurement sites across the study area. ESUs within a site are shown in a 10-m resolution false-color-composited map based on the Sentinel-2 data.

multispectral VIs. In this letter, the PROSAIL model [10] composed of PROSPECT-5B and 4SAIL is adopted to simulate the canopy reflectance. The biochemical and biophysical properties of wheat from our field measurements and other crops from the scientific literature are used as constraints on the model parameters. Leaf carotenoid content (*Car*) is linked to the leaf chlorophyll content (*Cab*) with a ratio of 1:5 based on the LOPEX'93 database [11]. The detailed values and ranges of the input parameters of the PROSAIL model are shown in Table I.

The spectra of the different types of soil from the Johns Hopkins University database are adopted as the background reflectance in the model. A total of 1000 simulated spectra of canopies with the LAI following the Gauss distribution are generated for evaluation, with leaf parameters randomly combined and other parameters fixed in their mean value of interval. Finally, the canopy spectral reflectance is integrated to the channel 4 (red) and 8 (near-infrared) spectral response functions of the Sentinel-2A MSI, the image of which is used to retrieve the LAI in Sections IV-B and IV-D.

B. In Situ LAI Measurements

The field LAI collection area is located in Hengshui, Hebei, China, which is in the middle of the North China Plain (centered at 115.79 °E, 37.77 °N; Fig. 1). The winter wheat is the main crops cultivated in this area from October of the present year to June of the succeeding year, and our field campaign was carried out on March 29–31 and May 4–6, 2017. Twenty-two 100 m × 100 m sites were established and evenly distributed across our study area in the homogeneous cropland. Five-elementary sampling units (ESUs) were set following a center-diagonal pattern in each site, and the distance between them within a site exceeded 50 m. The geographical coordinate of the ESU was recorded with a portable GPS. The LAI data were collected five times in each ESU by using the LAI-2000 Plant Canopy Analyzer within an approximately 5-m radius area centered at the ESU point. The median of the five measurements was considered as the final LAI value for the specific ESU, and the standard deviation of five measurements in an ESU was regarded as the uncertainty, which varied from 0.15 to 0.78. According to the adopted equipment and the working scheme of our field campaign, the LAI used in this letter should be understood as the effective PAI.

C. Sentinel-2A Multispectral Imagery

The MSI imagery of Sentinel-2A includes 13 bands, and the red (band 4) and near-infrared (band 8) bands used for computing the VIs have a spatial resolution of 10 m. These data can be downloaded freely from the Sentinels Scientific Data Hub (http://scihub.copernicus.eu/) as Level-1C orthorectified reflectance at top of the atmosphere. An atmospheric correction was conducted using the Sen2Cor atmospheric correction toolbox (version 2.4.0) built into the Sentinel Application Platform software (version 5.0.0) to obtain the surface reflectance [12].

III. METHOD

A. Inverted Difference Vegetation Index

The reflectance for vegetative canopies is relatively low in the red (660–690 nm) and high in the near-infrared (780–1100 nm) domain. Such values characterize the canopy's major feature against the reflectance spectra of other objects. Thus, $1-\rho_{\text{red}}$ can represent the high absorption plus the transmittance in the red domain and $1-\rho_{\text{nir}}$ represents the low absorption plus transmittance in the near-infrared domain of the spectrum because of the effect of leaf pigments in the vegetation to a certain extent [13]. To enhance this difference in the absorptive and reflective properties of the canopy in the red and near-infrared domains, the IDVI was developed for a large LAI estimation. The relevant formula is shown as follows:

$$\text{IDVI} = \frac{(1-\rho_{\text{red}})+\rho_{\text{nir}}}{(1-\rho_{\text{nir}})+\rho_{\text{red}}} = \frac{1+(\rho_{\text{nir}}-\rho_{\text{red}})}{1-(\rho_{\text{nir}}-\rho_{\text{red}})} \quad (1)$$

where ρ_{red} and ρ_{nir} refer to the surface reflectance of the red and near-infrared bands, respectively.

The spectral reflectance of the background soil is relatively high in the red band and low in the near-infrared band compared with those of vegetation. Thus, the IDVI of the background soil may possess a larger denominator value and a smaller numerator value compared with those of vegetation, which greatly reduces its value compared with that of vegetation. The reflectance of surface water in the red and near-infrared bands is very low, and the former is slightly larger; hence, the IDVI of water is slightly lower than 1. Similarly, some high-reflecting objects, such as snow

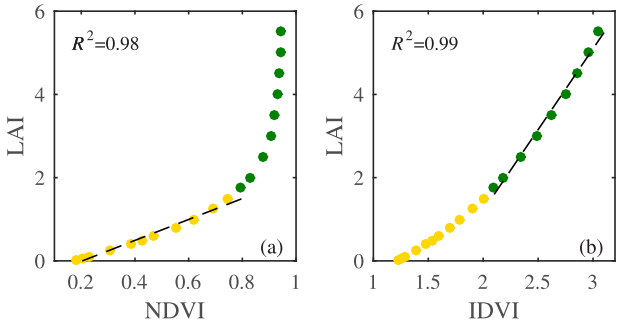

Fig. 2. Relationship between (a) LAI and NDVI and (b) LAI and IDVI. Yellow dots: sparse vegetation. Green dots: dense vegetation.

and clouds, characterize high reflectance in the red and near-infrared bands, leading to the IDVI values close to 1. Thus, such objects can be easily distinguished from that of vegetation with the IDVI. For dense vegetation, the absorption in the red band and the reflectance in the near-infrared band are both higher than those of sparse vegetation. While the increment of the reflectance of near-infrared band narrows down gradually, the denominator value is small enough at this time to boost the slight difference in the signal, which magnifies the IDVI increment for dense vegetation.

Based on the mean value of each parameter in Table I, the simulated canopy spectrum is generated to illustrate the relationship between the NDVI or IDVI and the LAI (Fig. 2). In this regard, large LAIs present a more stable and lower sloped linear relationship with the IDVI than those with the NDVI.

B. Statistical Model Based on the IDVI and NDVI

The NDVI has a fairly stable statistical relationship with the LAI in low-value ranges [14]; thus, we considered the NDVI-based relationship as the LAI estimation method in the sparse-vegetation conditions. An IDVI-based relationship is mainly adopted in large LAIs. To increase the accuracy and stability of the LAI estimation results by combining the NDVI and IDVI, we introduced the logic function as a dynamic scale factor as follows:

$$\alpha = \frac{1}{1 + e^{-k(\mathrm{NDVI} - \mathrm{NDVI}_t)}} \tag{2}$$

where NDVI_t is the threshold value of the NDVI upon saturation, which could usually be assigned a default value of 0.8 based on [15] and [16] and our experiment results (see Fig. 2), and k is the amplitude factor in the logic function. When NDVI_t is a slightly off 0.8 due to its uncertainty in practical applications, the scale factor does not deviate from 0.5 markedly. However, when the NDVI deviates from the threshold to a certain extent, the index adopted in the sparse-vegetation (NDVI) or dense-vegetation (IDVI) conditions should take the dominate place in the overall LAI estimation. Consequently, k is ideally set at 12–20 based on the above-mentioned criteria. Given variations in the crop type and other influencing factors, NDVI_t should be updated by *a priori* knowledge before the model is applied to a new region.

Thus, the final LAI estimation equation is as follows:

$$\mathrm{LAI}_{\mathrm{estimation}} = (1 - \alpha)\mathrm{LAI}_{\mathrm{NDVI}} + \alpha \mathrm{LAI}_{\mathrm{IDVI}} \tag{3}$$

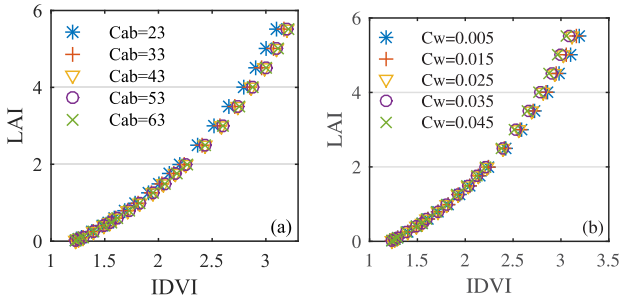

Fig. 3. Relationship between the IDVI and LAI under different (a) chlorophyll content and (b) water contents.

where $\mathrm{LAI}_{\mathrm{NDVI}}$ and $\mathrm{LAI}_{\mathrm{IDVI}}$ are the LAI estimation results from the statistical model fit by a linear function based on the NDVI and IDVI separately in the appropriate LAI levels.

The estimation result is based on the weighted average of the outcome from the NDVI and IDVI, and the weighted factor varies with the vegetation coverage density. The NDVI is more sensitive than the IDVI in the sparse vegetation, because the former changes significantly with the increase in LAI. Thus, the scale factor α is close to 0 for most sparse crop fields, and the NDVI is much lower than the threshold. Thus, the NDVI is highly weighted in the overall LAI estimation model in this domain. When the NDVI increases and approaches the saturation threshold, α increases rapidly to 0.5. Then, when the NDVI is crossing and deviating from the threshold value, α increases rapidly to 1 and the IDVI would become the major contributor in the LAI estimating model.

IV. Analysis and Discussion

A. Sensitivity Analysis

To ensure the accuracy and robustness of our LAI retrieval model, the VIs adopted should be sensitive to the LAI but not to other influencing factors. Chlorophyll and water are the most essential absorptive materials in the leaves of crops, and their concentrations vary widely in different phenological stages, which may greatly affect the reflectance spectra [17]. As such, we focus on the leaf water and chlorophyll content in our sensitivity study. Other parameters that do not vary much in a particular cropland are also considered in our sensitivity analysis discussions to provide more information.

Fig. 3 shows the relationship between the LAI and the IDVI under different chlorophyll and water contents based on the simulated data with the PROSAIL model. The IDVI was extremely stable under different chlorophyll [see Fig. 3(a)] and water [see Fig. 3(b)] contents in small and large LAIs, which means that the influence of these factors on the IDVI value is fairly weak in a specific leaf area condition. The same property is also observed for the NDVI in [18] and [19].

Among other influencing factors, including leaf property, canopy structure, observation geometry, and background soil types, the average leaf angle affects the stability of the IDVI the most, especially in the large LAI domains. The influence of the background soil type is more significant in the small LAIs than that in the large LAIs. However, the large LAIs are the most often applied interval of the IDVI in the proposed model. Thus, soil influence could be minimized to some extent. Sun and viewing geometry also slightly affect the IDVI according to our experimental results.

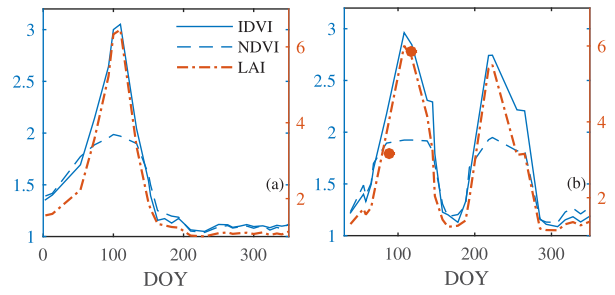

Fig. 4. Time series plot of the IDVI, NDVI, and LAI on (a) one of the BELMANIP sites and (b) Hengshui field campaign ESU. The orange dots in (b) is the *in situ* LAI observations.

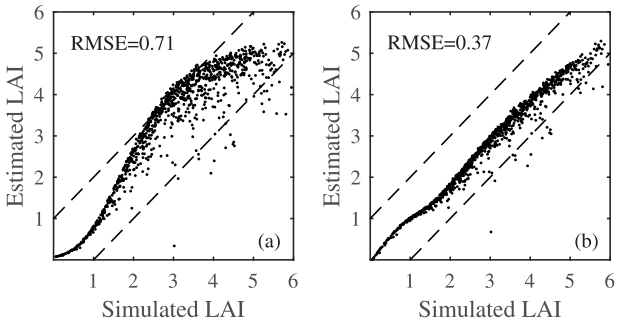

Fig. 5. Comparison of estimated and simulated LAIs using (a) NDVI model and (b) proposed model.

The average leaf angle represents the canopy structure of a specific type of crop. While its sensitivity could limit the usage of the IDVI in vast areas with complex crop types, it is acceptable in regional scale applications, because the major crop type is identical and constant over a specific area and period.

B. Time-Series Analysis

The time series curves of the LAI are plotted at two typical crop sites throughout 2017 and compared with those of the NDVI and IDVI (see Fig. 4). The first crop site, located in Southern France (48.81 °N, 4.71 °E), was chosen from BELMANIP site database, and the second site is a Hengshui field campaign ESU (37.31 °N, 115.88 °E). *In situ* LAI observations for the Hengshui ESU are represented by orange dots in Fig. 4(b). The shape of the VI curves seems similar in the small LAIs. However, when the LAI increases, the NDVI becomes saturated and remains constant. By comparison, the results of the IDVI continue to increase and demonstrate a wider variation range in accordance with the LAI changes.

C. Evaluation by Using Simulated Data

To evaluate the performance of our proposed LAI retrieval method, we select the most widely used NDVI-based regression model for comparison [20], [21]. Using the data in Fig. 2, the exponential function, which features the best fitting formation of the NDVI-based model, could be written as follows:

$$\mathrm{LAI} = 0.0066e^{7.42\mathrm{NDVI}} \tag{4}$$

Given the evaluation results (see Fig. 5) of the simulated data, we discover that the traditional regression model performs well in the sparse-vegetation section (LAI $<$ 2).

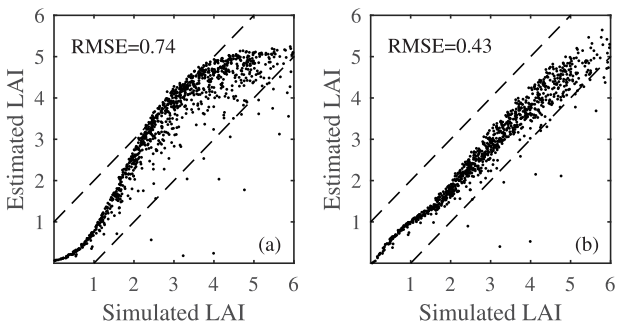

Fig. 6. Comparison of estimated and simulated LAIs using (a) NDVI model and (b) proposed model by adding a maximum 5% random noise.

However, the LAI is overestimated in the medium vegetation coverage condition (2 $<$ LAI $<$ 5) and underestimated in the dense-vegetated condition (LAI $>$ 5). The overall root mean square error (RMSE) is 0.71, and 85.80% of the samples remain within the ± 1 interval of the 1:1 line. By contrast, the proposed model performs effectively for the entire LAI range (RMSE = 0.37, 96.90% of the samples in the interval).

Considering the influence of soil types, sensor spectral responses, and atmospheric and terrain effects, similar LAI conditions may appear different in remote sensing imageries [22]. To test the robustness of our model, we added a maximum of 5% random disturbance to the red and near-infrared reflectances of the Sentinal-2A MSI. Results (see Fig. 6) show that the RMSE increases slightly for both models. The samples retained within the ± 1 interval of the 1:1 line are 85.20% and 96.40% for the NDVI model and the proposed model, respectively, which is similar to the previous overall accuracy observed.

Given the above results, we determine that our proposed model, which combined NDVI and IDVI, achieves a high level of consistency with the simulated LAI. This observation suggests the potential robust applicability of the model.

D. Validation by Using In Situ Observation Data

The proposed model is applied to the Sentinel-2 MSI data and cross-validated with *in situ* LAI observations. The imageries used for validation were acquired on March 29 and April 28, approximately in accordance with the fieldwork time arrangement. The LAI estimation result is compared with the traditional statistical models based on single VIs (i.e., NDVI, SAVI, and IDVI). Based on the outlier-removed *in situ* LAI measurements and near-simultaneous Sentinel-2A imageries, the relationship of VIs (NDVI, SAVI, and IDVI) with the LAI is shown in Fig. 7. The NDVI (R^2 = 0.63) and the SAVI (R^2 = 0.75) display a nonlinear relationship with the LAI. The NDVI becomes saturated when the LAI is higher than 4, and the SAVI performs slightly better than the NDVI. The IDVI achieves the strongest linear correlation with the LAI in the whole interval investigated ($R^2 = 0.82$).

Table II reveals the estimation accuracy of different statistical regression methods. The regression methods on the NDVI and SAVI are constructed by their best fit exponential relationship with the LAI. The RMSE of the NDVI model is the highest (1.15) among the values obtained from the models tested, because the saturation effect is quite explicit

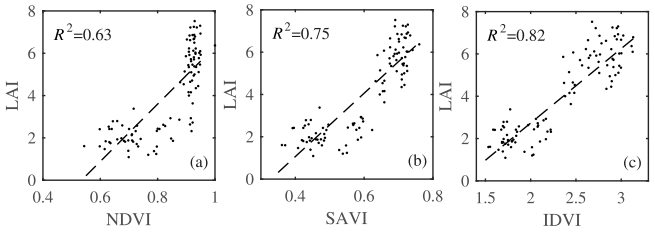

Fig. 7. Relationship between (a) NDVI and LAI, (b) SAVI and LAI, and (c) IDVI and LAI based on the *in situ* LAI observations.

TABLE II
ESTIMATION ACCURACY OF DIFFERENT LAI RETRIEVAL MODELS

Method	R	RMSE
Exponential regression on NDVI	0.84	1.15
Exponential regression on SAVI	0.90	0.89
Linear regression on IDVI	0.90	0.85
Proposed model on NDVI and IDVI	0.91	0.81

(see Fig. 7). The SAVI model overcomes the saturation issue to some extent, and the estimated RMSE decreases to 0.91. The model based on a single IDVI shows a performance similar to that of the SAVI model, and the proposed method on the NDVI and IDVI offers the highest prediction ability with $R = 0.91$ and RMSE $= 0.81$.

The uncertainty of the measurements, especially in the large LAIs, remains a major issue of validation, thus weakening the effectiveness of the validation results. Only one crop type was used for validation; hence, case-specific calibration is required for future applications.

V. CONCLUSION

In this letter, a new VI called IDVI is proposed from the red and near-infrared surface reflectances to retrieve the crop LAI in the dense-vegetated areas. Based on our sensitivity and time series analysis results, the IDVI is insensitive to leaf biochemical parameters and has a wider variation range than the NDVI. By exploiting the stability of the NDVI in the sparse-vegetated conditions and the nonsaturation of the IDVI in dense-vegetated conditions, we constructed a novel statistical model based on the NDVI and IDVI with a dynamic scale factor to estimate crop LAIs. Evaluation and validation results based on the simulated spectra and Sentinel-2 imageries demonstrated that our new statistical retrieval method is more accurate and robust than the existing regression models based on a single VI in the crop LAI estimation. However, parameter recalibration is required for applications in a new region, and additional work remains necessary in terms of validations under different remote sensing imageries and crop or vegetation types.

ACKNOWLEDGMENT

The authors would like to thank the Sentinel Scientific Data Hub for providing Sentinel-2A MSI data and the software and algorithm for atmospheric correction.

REFERENCES

[1] K. Richter, C. Atzberger, F. Vuolo, P. Weihs, and G. D'Urso, "Experimental assessment of the sentinel-2 band setting for RTM-based LAI retrieval of sugar beet and maize," *Can. J. Remote Sens.*, vol. 35, no. 3, pp. 230–247, 2009.

[2] M. Weiss, F. Baret, G. J. Smith, I. Jonckheere, and P. Coppin, "Review of methods for *in situ* leaf area index (LAI) determination: Part II. Estimation of LAI, errors and sampling," *Agricult. Forest Meteorol.*, vol. 121, nos. 1–2, pp. 37–53, Jan. 2004.

[3] G. Papadavid, D. G. Hadjimitsis, L. Toulios, and S. Michaelides, "Mapping potato crop height and leaf area index through vegetation indices using remote sensing in Cyprus," *J. Appl. Remote Sens.*, vol. 5, no. 1, p. 3526, Jan. 2011.

[4] J. Verrelst *et al.*, "Optical remote sensing and the retrieval of terrestrial vegetation bio-geophysical properties—A review," *ISPRS J. Photogram. Remote Sens.*, vol. 108, pp. 273–290, Oct. 2015.

[5] S. Potithep, S. Nagai, K. N. Nasahara, H. Muraoka, and R. Suzuki, "Two separate periods of the LAI–VIs relationships using *in situ* measurements in a deciduous broadleaf forest," *Agricult. Forest Meteorol.*, vol. 169, pp. 148–155, Feb. 2013.

[6] G. Yang, C. Zhao, Q. Liu, W. Huang, and J. Wang, "Inversion of a radiative transfer model for estimating forest LAI from multisource and multiangular optical remote sensing data," *IEEE Trans. Geosci. Remote Sens.*, vol. 49, no. 3, pp. 988–1000, Mar. 2011.

[7] R. Colombo, D. Bellingeri, D. Fasolini, and C. M. Marino, "Retrieval of leaf area index in different vegetation types using high resolution satellite data," *Remote Sens. Environ.*, vol. 86, no. 1, pp. 120–131, Jun. 2003.

[8] H. Chen, Z. Niu, W. Huang, and J. Feng, "Predicting leaf area index in wheat using an improved empirical model," *J. Appl. Remote Sens.*, vol. 7, no. 1, p. 3577, Apr. 2013.

[9] F. Baret and G. Guyot, "Potentials and limits of vegetation indices for LAI and APAR assessment," *Remote Sens. Environ.*, vol. 35, nos. 2–3, pp. 161–173, Feb./Mar. 1991.

[10] K. Berger *et al.*, "Evaluation of the PROSAIL model capabilities for future hyperspectral model environments: A review study," *Remote Sens.*, vol. 10, no. 1, p. 85, Jan. 2018.

[11] B. Hosgood, S. Jacquemoud, G. Andreoli, J. Verdebout, A. Pedrini, and G. Schmuck, "Leaf optical properties experiment 93 (LOPEX93)," Joint Research Centre/IPSC/SERAC Unit, Ispra, Italy, Tech. Rep. EUR 16095 EN, 1994.

[12] F. Vuolo *et al.*, "Data service platform for sentinel-2 surface reflectance and value-added products: System use and examples," *Remote Sens.*, vol. 8, no. 11, p. 938, Nov. 2016.

[13] D. A. Sims and J. A. Gamon, "Relationships between leaf pigment content and spectral reflectance across a wide range of species, leaf structures and developmental stages," *Remote Sens. Environ.*, vol. 81, nos. 2–3, pp. 337–354, Aug. 2002.

[14] L. Fan, Y. Gao, H. Brück, and C. Bernhofer, "Investigating the relationship between NDVI and LAI in semi-arid grassland in Inner Mongolia using *in-situ* measurements," *Theor. Appl. Climatol.*, vol. 95, no. 1, pp. 151–156, Jan. 2009.

[15] A. A. Gitelson, "Wide dynamic range vegetation index for remote quantification of biophysical characteristics of vegetation," *J. Plant Physiol.*, vol. 161, no. 2, pp. 165–173, 2004.

[16] Y. Gu, B. K. Wylie, D. M. Howard, K. P. Phuyal, and L. Ji, "NDVI saturation adjustment: A new approach for improving cropland performance estimates in the Greater Platte River Basin, USA," *Ecological Indicators*, vol. 30, pp. 1–6, Jul. 2013.

[17] Y. Peng and A. A. Gitelson, "Remote estimation of gross primary productivity in soybean and maize based on total crop chlorophyll content," *Remote Sens. Environ.*, vol. 117, no. 1, pp. 440–448, Feb. 2012.

[18] P. J. Zarco-Tejada *et al.*, "Assessing vineyard condition with hyperspectral indices: Leaf and canopy reflectance simulation in a row-structured discontinuous canopy," *Remote Sens. Environ.*, vol. 99, no. 3, pp. 271–287, Nov. 2005.

[19] C. Wu, L. Wang, Z. Niu, S. Gao, and M. Wu, "Nondestructive estimation of canopy chlorophyll content using Hyperion and Landsat/TM images," *Int. J. Remote Sens.*, vol. 31, no. 8, pp. 2159–2167, 2010.

[20] B. Duchemin *et al.*, "Monitoring wheat phenology and irrigation in Central Morocco: On the use of relationships between evapotranspiration, crops coefficients, leaf area index and remotely-sensed vegetation indices," *Agricult. Water Manage.*, vol. 79, no. 1, pp. 1–27, Jan. 2006.

[21] C. L. Wiegand *et al.*, "Multisite analyses of spectral-biophysical data for wheat," *Remote Sens. Environ.*, vol. 42, no. 1, pp. 1–21, Oct. 1992.

[22] G. Yin *et al.*, "Improving leaf area index retrieval over heterogeneous surface by integrating textural and contextual information: A case study in the Heihe river basin," *IEEE Geosci. Remote Sens. Lett.*, vol. 12, no. 2, pp. 359–363, Feb. 2015.